

# Structure-Property Relationships of Short Chain (Mixed) Cellulose Esters Synthesized in a DMSO/TMG/CO<sub>2</sub> Switchable Solvent System

Timo Sehn,<sup>†</sup> Michael A. R. Meier<sup>\*,‡,†</sup>

<sup>†</sup> Institute of Biological and Chemical Systems – Functional Molecular Systems (IBCS-FMS), Karlsruhe Institute of Technology (KIT), 76131 Karlsruhe, Germany

<sup>‡</sup> Institute of Organic Chemistry (IOC), Materialwissenschaftliches Zentrum (MZE), Karlsruhe Institute of Technology (KIT), Straße am Forum 7, 76131 Karlsruhe, Germany

## Abstract

Increasing environmental pollution and petroleum resource depletion are important indicators for the inevitable replacement of fossil-based polymeric materials with more sustainable counterparts. Hence, the development of bio-based materials from renewable resources, such as cellulose, is of great importance. Herein, we introduce a rapid and homogenous microwave assisted synthesis of high molecular weight ( $59 \text{ kDa} \leq M_n \leq 116 \text{ kDa}$ ) short chain (mixed) cellulose esters (CEs) with variable acyl side chain length ( $2 \leq C \leq 8$ ) by using a DMSO/TMG/CO<sub>2</sub> switchable solvent system. Accordingly, (mixed) CEs were synthesized by implementing tetramethylguanidine (TMG) into a switchable solvent system (DMSO/TMG/CO<sub>2</sub>) and simple variation of reaction parameters, followed by in-depth structural characterization via IR, <sup>1</sup>H NMR, <sup>13</sup>C NMR and SEC. Examination of the structure-property relationships revealed a decrease in the glass transition temperature ( $177 \text{ °C} \leq T_g \leq 204 \text{ °C}$ ), an increase in surface hydrophobicity, i.e. water contact angle (WCA) ( $65^\circ \leq \text{WCA} \leq 98^\circ$ ) and a decrease of young's modulus ( $7.51 \text{ MPa} \leq E \leq 13.6 \text{ MPa}$ ), with longer alkyl side chains.

## Keywords

cellulose ester, switchable solvent system, tetramethylguanidine, structure property relationships

## INTRODUCTION

A critical consideration of petroleum resource depletion, environmental pollution and future food shortages underlines the required replacement of fossil based polymeric materials by renewable counterparts.<sup>1,2,3</sup> Cellulose, as the most abundant biopolymer on earth (natural production of  $1.5 \times 10^{12}$  tons p.a.),<sup>4,5</sup> possesses unique properties, i.e., biodegradability, biocompatibility, high thermal and mechanical stability,<sup>6,7</sup> and hence plays a key role in sustainable material development. Although, cellulose has been recognized as a raw material for nearly 170 years,<sup>4,8,9</sup> its efficient modification remains challenging, due to the limited processibility and insolubility of cellulose in common organic solvents.<sup>7,9,10</sup> The aforementioned phenomena, i.e. limited processability and solubility, arise from the chemical structure of cellulose, which consists of glucose units linked by  $\beta$ -glycosidic bonds.<sup>11</sup> More precisely, extensive intra- and intermolecular hydrogen bonding between hydroxyl groups strongly limit the potential for modification and application.<sup>11,12</sup> Nevertheless, in recent years, different heterogenous and homogenous approaches for cellulose modifications have been established. Heterogenous derivatizations of cellulose, i.e. in solid or swollen form, is more practical and therefore applied for most commercially available cellulose derivatives, such as exemplarily cellulose esters (CEs).<sup>13,14,15</sup> However, the previously described and industrially deployed modification processes, i.e. heterogenous ones, reveal challenges concerning the degradation of the cellulose backbone and control of the degree of substitution (DS).<sup>5,13,16</sup> On the contrary, homogenous modification approaches of cellulose achieve a better control of the DS and thus enable a tailor-made adjustment of the materials properties.<sup>5,8,17</sup> Up to the present day, various systems for a homogenous derivatization of cellulose have been investigated using solvents such as *N*-methylmorpholine *N*-oxide,<sup>18,19</sup> dimethyl sulfoxide-tetrabutylammonium fluoride (DMSO-TBAF),<sup>20</sup>  $\text{LiClO}_4 \cdot 3 \text{H}_2\text{O}$  molten salt hydrate,<sup>21</sup> *N,N*-dimethylacetamide-lithiumchloride (DMAc-LiCl)<sup>22,23</sup> or ionic liquids (ILs), e.g. 1-allyl-3-methylimidazolium chloride,<sup>24,25</sup> 1-butyl-3-methylimidazolium chloride (BMIMCl)<sup>26</sup> or 1-ethyl-3-methylimidazolium 2-pyridinolate (EmimOPy).<sup>11</sup>

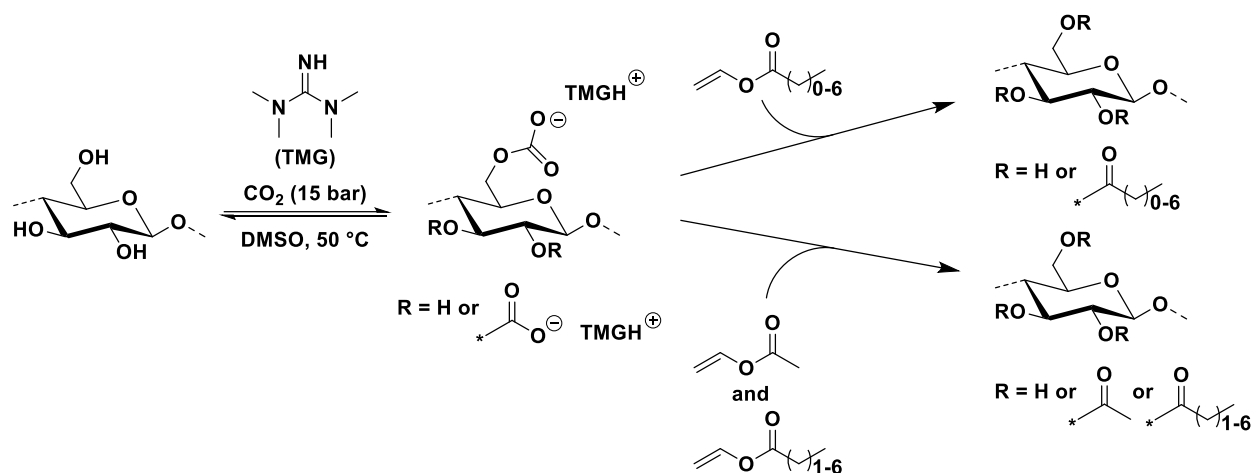
In 2013, Xie *et. al.* and Jérôme *et. al.* developed two novel, homogenous and reversible systems for cellulose dissolution containing carbon dioxide ( $\text{CO}_2$ ), a superbase, i.e. 1,8-diazabicyclo[5.4.0]undec-7-en (DBU) or 1,5,7-triazabicyclo[4.4.0]dec-5-en (TBD), and a polar aprotic solvent, i.e. dimethyl sulfoxide (DMSO).<sup>27,28</sup> The two methods are divided into the

so-called derivative approach, where cellulose is functionalized reversibly into a DMSO soluble ionic carbonate intermediate,<sup>28</sup> and the non-derivative approach, where an additional alcohol, e.g. methanol, hexanol or ethylene glycol, affords the formation of an ionic carbonate complex by the reaction with CO<sub>2</sub>.<sup>27</sup> Both approaches are based on the fundamental principle of the nonpolar-to-polar switchable solvent published by Jessop *et. al.* in 2005.<sup>29</sup> Crucially, the derivative switchable solvent system was frequently used for the synthesis of various cellulose derivatives, such as cellulose esters (CEs),<sup>5,7,30,31,32</sup> cellulose carbonates (CC),<sup>33</sup> cellulose thiocarbamates,<sup>34</sup> or cyanoethyl cellulose (CEC).<sup>9</sup>

From an industrial point of view, CEs are a commercially very important material class as they are already applied as biobased counterparts to fossil-based polymers in film, filter, food package, pharmaceutical, membrane and coating industries.<sup>3,6,7,10</sup> Thus, it is not surprising that CEs are already frequently investigated in the current literature, yet it is worth mentioning that the research interest in CE based materials was restricted for a long time to derivatives containing long acyl side chains.<sup>7,30,35,36</sup> The incorporation of side chains with increased length ( $C > 10$ ) of fatty acyl groups onto the cellulose backbone affords an internal plasticizer effect and thus enables an improved melt processability, which is an important requirement for industrial applicability.<sup>3,6</sup> However, thermal and mechanical properties of the aforementioned materials remain critical, as they reveal mostly low strength and brittleness.<sup>3,37,38</sup> On the contrary, short chain CEs ( $C \leq 8$ ) reveal improved materials properties, i.e. thermal and mechanical stability, but suffer simultaneously a limited processability resulting from the extensive intra- and intermolecular interactions, i.e. hydrogen bonding, between the cellulose backbone.<sup>6</sup> Recently, Vodovotz *et. al.* examined the thermal and barrier properties of short chain cellulose triesters (CTEs) depending on their side chain length, suggesting possible applications in food packaging.<sup>6</sup> In order to overcome the aforementioned challenges, in other words to combine processability and acceptable materials properties, Iji *et. al.* and Zhang *et. al.* established additional approaches for the synthesis of mixed CEs in 2017 and 2018, respectively.<sup>3,10</sup> Particularly, the influence of combining short ( $C = 2$ ) and long ( $C < 15$ ) acyl side chains as well as the combination of bulky and non-bulky acyl side groups (such as exemplarily aromatic ones with acetyl moieties) were investigated, respectively.

In line with the aforementioned challenges, we herein introduce a rapid homogenous microwave assisted synthesis of high molecular weight short chain (mixed) CEs with variable acyl side chain length ( $2 \leq C \leq 8$ ) and in a DS range of 1.99 to 2.34 by using a DMSO/TMG/CO<sub>2</sub> switchable

solvent system (Scheme 1). Accordingly, two polymer libraries (Scheme 2) were synthesized and in-depth characterized regarding their chemical structures (via.  $^1\text{H}$  NMR, IR, and SEC), and structure property relationship investigations (via DSC, TGA, WCA and tensile strength) were performed.



**Scheme 1.** Cellulose dissolution in DMSO/TMG/ $\text{CO}_2$  switchable solvent system and subsequent transesterification reaction towards short chain (mixed) CEs. Top: CEs of different chain lengths are obtained; bottom: mixed CEs containing acetate moieties and one more, different ester, are obtained.

## EXPERIMENTAL SECTION

### Materials

Microcrystalline cellulose (MCC, Sigma Aldrich) was dried under reduced pressure at 100 °C for 24 hours prior to use. Dimethyl sulfoxide (DMSO, dried and stored over molecular sieve, Acros Organics, >99.7%), vinyl acetate (Sigma Aldrich, >99%), vinyl propionate (TCI, >98%), vinyl butyrate (TCI, >98%), vinyl valerate (Sigma Aldrich, 97%), vinyl hexanoate (TCI, 99%), vinyl octanoate (TCI, >99%), tetramethylguanidine (TMG, TCI, >99%), DMSO-*d*<sub>6</sub> (Eurisotop, 99.8%), CDCl<sub>3</sub> (Eurisotop, 99.8%), pyridine (Sigma Aldrich, 99.8%) were used without further purification. All other solvents were employed in technical grade.

### General Procedure for the Synthesis of Short Chain CEs

In a microwave vial, microcrystalline cellulose (MCC, 0.10 g, 0.62 mmol) was suspended in 3.33 mL anhydrous DMSO followed by the dropwise addition of TMG (0.93 mL, 0.86 g, 7.44 mmol, 12.0 equiv. per AGU). Subsequently, a CO<sub>2</sub> atmosphere (15 bar) was applied in a pressure reactor for 30 minutes at 50 °C until a homogeneous solution was obtained. The corresponding vinyl ester (7.44 mmol, 12.0 equiv. per AGU) was then added and the transparent reaction mixture was subjected to microwave irradiation (300W) for 10 minutes at 140 °C. The desired CEs were precipitated under vigorous stirring in 60 mL isopropanol (or isopropanol/water mixture 3:1 wt% for CH and CO) and filtrated. In order to remove residual impurities and DMSO, the products were additionally stirred in 80 mL isopropanol under reflux for 1 h, vacuum filtrated and dried overnight under reduced pressure at 100 °C. The final products were obtained as white powdery solids. The corresponding yields were determined according to Eqn. S3 (based on DS<sub>1H</sub>) and ranged from 46 to 73%.

**CA:** ATR-IR:  $\nu$  (cm<sup>-1</sup>) = 3126 - 3711  $\nu$  (O-H), 2812 - 3033  $\nu$  (C-H), 1738  $\nu$  (C=O), 1225  $\nu$  (C-O<sub>ester</sub>), 1034  $\nu$  (C-O<sub>AGU</sub>). <sup>1</sup>H NMR (400 MHz, DMSO-*d*<sub>6</sub>)  $\delta$  (ppm) = 5.37 – 2.88 (m, AGU, 7H), 2.20 – 1.63 (m, H<sub>a</sub>, 3H).

**CP:** ATR-IR:  $\nu$  (cm<sup>-1</sup>) = 3094 - 3664  $\nu$  (O-H), 2840 - 3041  $\nu$  (C-H), 1738  $\nu$  (C=O), 1164  $\nu$  (C-O<sub>ester</sub>), 1061  $\nu$  (C-O<sub>AGU</sub>). <sup>1</sup>H NMR (400 MHz, DMSO-*d*<sub>6</sub>)  $\delta$  (ppm) = 5.30 – 2.76 (m, AGU, 7H), 2.43 – 1.83 (m, H<sub>b</sub>, 2H), 1.29 – 0.43 (m, H<sub>a</sub>, 3H).

**CB:** ATR-IR:  $\nu$  (cm<sup>-1</sup>) = 3062 - 3674  $\nu$  (O-H), 2772 - 3039  $\nu$  (C-H), 1733  $\nu$  (C=O), 1162  $\nu$  (C-O<sub>ester</sub>), 1038  $\nu$  (C-O<sub>AGU</sub>). <sup>1</sup>H NMR (400 MHz, DMSO-*d*<sub>6</sub>)  $\delta$  (ppm) = 5.32 – 2.75 (m, AGU, 7H), 2.39 – 1.84 (m, H<sub>c</sub>, 2H), 1.54 (br, H<sub>b</sub>, 2H), 0.88 (br, H<sub>a</sub>, 3H).

**CV:** ATR-IR:  $\nu$  ( $\text{cm}^{-1}$ ) = 3083 - 3667  $\nu$  (O-H), 2787 - 3027  $\nu$  (C-H), 1733  $\nu$  (C=O), 1160  $\nu$  (C-O<sub>ester</sub>), 1032  $\nu$  (C-O<sub>AGU</sub>). <sup>1</sup>H NMR (400 MHz, DMSO-*d*<sub>6</sub>)  $\delta$  (ppm) = 5.42 – 2.78 (m, AGU, 7H), 2.40 – 1.86 (m, H<sub>d</sub>, 2H), 1.47 (br, H<sub>c</sub>, 2H), 1.28 (br, H<sub>b</sub>, 2H), 0.85 (br, H<sub>a</sub>, 3H).

**CH:** ATR-IR:  $\nu$  ( $\text{cm}^{-1}$ ) = 3068 - 3680  $\nu$  (O-H), 2783 - 3033  $\nu$  (C-H), 1738  $\nu$  (C=O), 1158  $\nu$  (C-O<sub>ester</sub>), 1032  $\nu$  (C-O<sub>AGU</sub>). <sup>1</sup>H NMR (400 MHz, DMSO-*d*<sub>6</sub>)  $\delta$  (ppm) = 5.38 – 2.83 (m, AGU, 7H), 2.39 – 1.84 (m, H<sub>d</sub>, 2H), 1.49 (br, H<sub>c</sub>, 2H), 1.25 (br, H<sub>b</sub>, 4H), 0.85 (br, H<sub>a</sub>, 3H).

**CO:** ATR-IR:  $\nu$  ( $\text{cm}^{-1}$ ) = 3113 - 3667  $\nu$  (O-H), 2769 - 3040  $\nu$  (C-H), 1738  $\nu$  (C=O), 1155  $\nu$  (C-O<sub>ester</sub>), 1034  $\nu$  (C-O<sub>AGU</sub>). <sup>1</sup>H NMR (400 MHz, DMSO-*d*<sub>6</sub>)  $\delta$  (ppm) = 5.42 – 2.93 (m, AGU, 7H), 2.37 – 1.89 (m, H<sub>d</sub>, 2H), 1.49 (br, H<sub>c</sub>, 2H), 1.25 (br, H<sub>b</sub>, 8H), 0.84 (br, H<sub>a</sub>, 3H).

### General Procedure for the Synthesis of Short Chain Mixed CEs

In a microwave vial, microcrystalline cellulose (MCC, 0.10 g, 0.62 mmol) was suspended in 3.33 mL DMSO (anhydrous 99.9%) followed by the dropwise addition of TMG (0.93 mL, 0.86 g, 7.44 mmol, 12.0 equiv. per AGU). After transferring the reaction mixture into a pressure reactor, a CO<sub>2</sub> atmosphere (15 bar) was applied for 30 minutes at 50°C until a transparent yellowish solution was obtained. Subsequently, vinyl acetate (0.34 mL, 0.32 g, 3.72 mmol, 6.00 equiv. per AGU) as well as the corresponding second vinyl ester (3.72 mmol, 6.00 equiv. per AGU) were added and the transparent reaction mixture was subjected to microwave irradiation (300W) for 10 minutes at 140 °C. The desired CEs were precipitated under vigorous stirring in 60 mL isopropanol and filtrated. In order to remove residual impurities and DMSO, the products were additionally stirred in 80 mL isopropanol under reflux for 1 h, vacuum filtrated and dried overnight under reduced pressure at 100 °C. The final products were obtained as white powdery solids. The corresponding yields were determined according to Eqn. S4 (based on DS<sub>1H</sub>) and ranged from 39 to 60%.

**CAP:** ATR-IR:  $\nu$  ( $\text{cm}^{-1}$ ) = 3144 – 3691  $\nu$  (O-H), 2778 - 3033  $\nu$  (C-H), 1731  $\nu$  (C=O), 1225  $\nu$  (C-O<sub>ester</sub>), 1162  $\nu$  (C-O<sub>S2</sub>), 1026  $\nu$  (C-O<sub>AGU</sub>). <sup>1</sup>H NMR (400 MHz, DMSO-*d*<sub>6</sub>)  $\delta$  (ppm) = 5.49 – 2.82 (m, AGU, 7H), 2.42 – 2.11 (m, H<sub>b</sub>, 2H), 2.10 – 1.60 (m, H<sub>a'</sub>, 3H), 1.02 (br, H<sub>a</sub>, 3H).

**CAB:** ATR-IR:  $\nu$  ( $\text{cm}^{-1}$ ) = 3115 – 3651  $\nu$  (O-H), 2807 - 3033  $\nu$  (C-H), 1731  $\nu$  (C=O), 1227  $\nu$  (C-O<sub>ester</sub>), 1165  $\nu$  (C-O<sub>S2</sub>), 1032  $\nu$  (C-O<sub>AGU</sub>). <sup>1</sup>H NMR (400 MHz, DMSO-*d*<sub>6</sub>)  $\delta$  (ppm) = 5.43 – 2.76 (m, AGU, 7H), 2.39 – 2.12 (m, H<sub>c</sub>, 2H), 2.10 – 1.68 (m, H<sub>a'</sub>, 3H), 1.52 (br, H<sub>b</sub>, 2H), 0.87 (br, H<sub>a</sub>, 3H).

**CAV:** ATR-IR:  $\nu$  ( $\text{cm}^{-1}$ ) = 3095 – 3674  $\nu$  (O-H), 2762 - 3033  $\nu$  (C-H), 1733  $\nu$  (C=O), 1223  $\nu$  (C-O<sub>ester</sub>), 1160  $\nu$  (C-O<sub>S2</sub>), 1028  $\nu$  (C-O<sub>AGU</sub>). <sup>1</sup>H NMR (400 MHz, DMSO-*d*<sub>6</sub>)  $\delta$  (ppm) = 5.41 – 2.75

(m, AGU, 7H), 2.40 – 2.12 (m, H<sub>d</sub>, 2H), 2.11 – 1.67 (m, H<sub>a'</sub>, 3H), 1.47 (br, H<sub>c</sub>, 2H), 1.27 (br, H<sub>b</sub>, 2H), 0.84 (br, H<sub>a</sub>, 3H).

**CAH:** ATR-IR:  $\nu$  (cm<sup>-1</sup>) = 3115 – 3686  $\nu$  (O-H), 2783 - 3033  $\nu$  (C-H), 1733  $\nu$  (C=O), 1223  $\nu$  (C-O<sub>ester</sub>), 1160  $\nu$  (C-O<sub>S2</sub>), 1030  $\nu$  (C-O<sub>AGU</sub>). <sup>1</sup>H NMR (400 MHz, DMSO-*d*<sub>6</sub>)  $\delta$  (ppm) = 5.34 – 2.77 (m, AGU, 7H), 2.40 – 2.14 (m, H<sub>d</sub>, 2H), 2.12 – 1.66 (m, H<sub>a'</sub>, 3H), 1.51 (br, H<sub>c</sub>, 2H), 1.26 (br, H<sub>b</sub>, 4H), 0.84 (br, H<sub>a</sub>, 3H).

**CAO:** ATR-IR:  $\nu$  (cm<sup>-1</sup>) = 3221 - 3686  $\nu$  (O-H), 2760 - 3033  $\nu$  (C-H), 1738  $\nu$  (C=O), 1223  $\nu$  (C-O<sub>ester</sub>), 1154  $\nu$  (C-O<sub>S2</sub>), 1028  $\nu$  (C-O<sub>AGU</sub>). <sup>1</sup>H NMR (400 MHz, DMSO-*d*<sub>6</sub>)  $\delta$  (ppm) = 5.44 – 2.83 (m, AGU, 7H), 2.39 – 2.12 (m, H<sub>d</sub>, 2H), 2.13 – 1.67 (m, H<sub>a'</sub>, 2H), 1.48 (br, H<sub>c</sub>, 2H), 1.22 (br, H<sub>b</sub>, 6H), 0.82 (br, H<sub>a</sub>, 3H).

## INSTRUMENTS

### Infrared Spectroscopy (IR)

Infrared spectra were recorded using a Bruker Alpha-p instrument with ATR technology in a range of  $\nu$  = 400–4000 cm<sup>-1</sup> with 24 scans per measurement and a resolution of 4 cm<sup>-1</sup>.

### Nuclear Magnetic Resonance (NMR) Spectroscopy

<sup>1</sup>H NMR spectra were recorded using a Bruker Ascend 400 MHz with 16 scans and a delay time *d*<sub>1</sub> of 5 seconds at 25 °C. The chemical shift was reported in ppm and referenced to the solvent signal of partly deuterated DMSO-*d*<sub>6</sub> at 2.50 ppm. <sup>13</sup>C NMR spectra were recorded using a Bruker Avance DRX at 126 MHz with 8192 scans and a delay time *d*<sub>1</sub> of 2 seconds at 25 °C. The signals were referenced to the solvent peak of partly deuterated DMSO-*d*<sub>5</sub> at 39.52 ppm.

### Size Exclusion Chromatography (SEC)

SEC measurements were performed in HFIP containing 0.1 wt% potassium trifluoroacetate (KTFA) using a Tosoh EcoSEC HLC8320 SEC system. The solvent flow was 0.40 mL min<sup>-1</sup> at 30 °C, and the concentration of the samples was 1 mg mL<sup>-1</sup>. The analysis was performed using a three-column system: PSS PFG Micro precolumn (3.0 × 0.46 cm, 10,000 Å), PSS PFG Micro (25.0 × 0.46 cm, 1000 Å), and PSS PFG Micro (25.0 × 0.46 cm, 100 Å). The system was calibrated with linear poly(methyl methacrylate) standards (Polymer Standard Service, Mp: 102– 981 kDa).

### Differential Scanning Calorimetry (DSC)

Thermal properties were measured on a TA DSC 2500 with a heating rate of 20 °C·min<sup>-1</sup> between -20 °C and 220 °C in TA Tzero sample holders. The glass transition temperature (*T*<sub>g</sub>) was

determined from the second heating run to eliminate possible interference from the polymer's thermal history.

### **Thermogravimetric Analysis (TGA)**

TGA measurements were carried out on the TA Instruments TGA 5500 under nitrogen atmosphere using platinum TGA sample pans and with a heating rate of  $10\text{ }^{\circ}\text{C min}^{-1}$  over a temperature range from 25 to  $500\text{ }^{\circ}\text{C}$ .

### **Water Contact Angel (WCA) Measurements**

Polymer films were spin cast (4000 rpm, 30 s, in air) from a polymer/pyridine solution ( $100\text{ }\mu\text{L}$ ,  $c = 1.67\text{ g mL}^{-1}$ ) onto a glass surface at ambient temperature. Contact angle measurements were performed with a DSA 25 contact angle goniometer (Krüss) using the sessile drop technique. A water droplet with a size of  $5\text{ }\mu\text{L}$  was slowly added onto the spin cast films by a micrometer syringe and contact angles of the spin cast films against the water droplet were measured. The average value of five measurements was calculated for each sample with a standard deviation less than 1.

### **Tensile strength measurement**

Polymer films were prepared by dissolving 100 mg of the respective material in 1.5 mL of pyridine and casting the solution into poly(tetrafluoro ethylene) plates (40 mm diameter). The solvent was evaporated overnight at room temperature. Subsequently, the polymer films were cut into dog bones (16 mm x 2 mm) and the thickness was determined with a digital vernier caliper. Tensile strength was measured using a Inspect table 10kN from Hegewald & Peschke with a 1.5 kN sensor. The initial speed was set to  $5\text{ mm min}^{-1}$  and three samples were analyzed for each ester.

### **Gas Chromatography-Mass Spectrometry (GC-MS)**

Gas chromatography-mass spectrometry (GC-MS) measurements were performed on a Varian 431 GC instrument with a HP-5 column ( $30\text{ m} \times 0.32\text{ mm} \times 0.25\text{ }\mu\text{m}$ ) and a Varian 210 ion trap mass detector. Scans were performed from 40 to 650  $m/z$  at a rate of  $1.0\text{ scan s}^{-1}$ . Initial temperature at  $95\text{ }^{\circ}\text{C}$  for 1 min, heating to  $220\text{ }^{\circ}\text{C}$  with a rate of  $15\text{ }^{\circ}\text{C min}^{-1}$ , heating to  $300\text{ }^{\circ}\text{C}$  with a rate of  $15\text{ }^{\circ}\text{C min}^{-1}$ , heating to  $325\text{ }^{\circ}\text{C}$  with a rate of  $15\text{ }^{\circ}\text{C min}^{-1}$ , retaining  $325\text{ }^{\circ}\text{C}$  for 3 min. The injector transfer line temperature was set to  $250\text{ }^{\circ}\text{C}$ . Measurements were performed with a split ratio of 50:1 using helium as carrier gas with a flow rate of  $1.0\text{ mL min}^{-1}$ .



## RESULTS AND DISCUSSION

CO<sub>2</sub> based switchable solvent systems evolved to a versatile tool for homogenous cellulose modifications.<sup>9,32,33,34</sup> These systems are typically based on superbases such as DBU or TBD and a polar aprotic co-solvent like DMSO.<sup>27,28</sup> Although the derivative approach (see above for details) is currently established as one of the most sustainable possibilities for homogenous cellulose modification, toxicity and expensiveness of the mainly employed superbases, i.e. DBU and TBD, remain as critical points.<sup>5</sup> Thus, the current work focuses on the investigation of a cheaper and nontoxic alternative, i.e. TMG, for cellulose dissolution and subsequent acylation in a CO<sub>2</sub> based switchable solvent system. As a first result, we observed that microcrystalline cellulose (MCC, 3 wt%) can be quantitatively dissolved within 30 minutes in the presence of TMG and DMSO when applying a CO<sub>2</sub> atmosphere of 15 bars (Figure S1). Having this information in hand, the subsequent transesterification reaction of cellulose with vinyl acetate (VA) to yield cellulose acetate (CA) was exemplarily studied. Based on previously reported systems for homogenous CA synthesis,<sup>5</sup> the first acylation reactions were conducted in a DMSO/TMG/CO<sub>2</sub> system under traditional heating conditions for 4 hours at 60 °C. In order to optimize the reaction conditions, different parameters, i.e. VA equivalents, TMG equivalents, heating method and reaction temperature, were investigated. Accordingly, the modification monitored by following the characteristic carbonyl vibration band at 1740 cm<sup>-1</sup> in ATR-IR spectra and additional DS<sub>1H</sub> determination via <sup>1</sup>H NMR spectroscopy. It is important to mention that, in order to afford comparability of all recorded IR spectra, a normalization to the unreacted C-O vibration band of the anhydroglucose unit (~ 1040 cm<sup>-1</sup>) was essential. Thus, first, the effect of VA and TMG equivalents were investigated, observing that the most promising results were obtained when VA and TMG were used in an equimolar ratio. Hence, the synthesis of CA-1, CA-2, and CA-3 were performed with 4.50/4.50, 6.00/6.00 and 9.00/9.00 equivalents of VA and TMG, respectively. Figure 1 reveals a gradual increase of the characteristic carbonyl vibration band around 1740 cm<sup>-1</sup> for CA-1, CA-2 and CA-3, respectively, indicating a more efficient cellulose modification when using increased VA and TMG equivalents (9.00/9.00 equiv.). The aforementioned trend is additionally underlined by an increase of DS<sub>1H</sub> from 0.80 (CA-1, Figure S2 and Table S1) to 1.51 (CA-3, Figure S4 and Table S1).

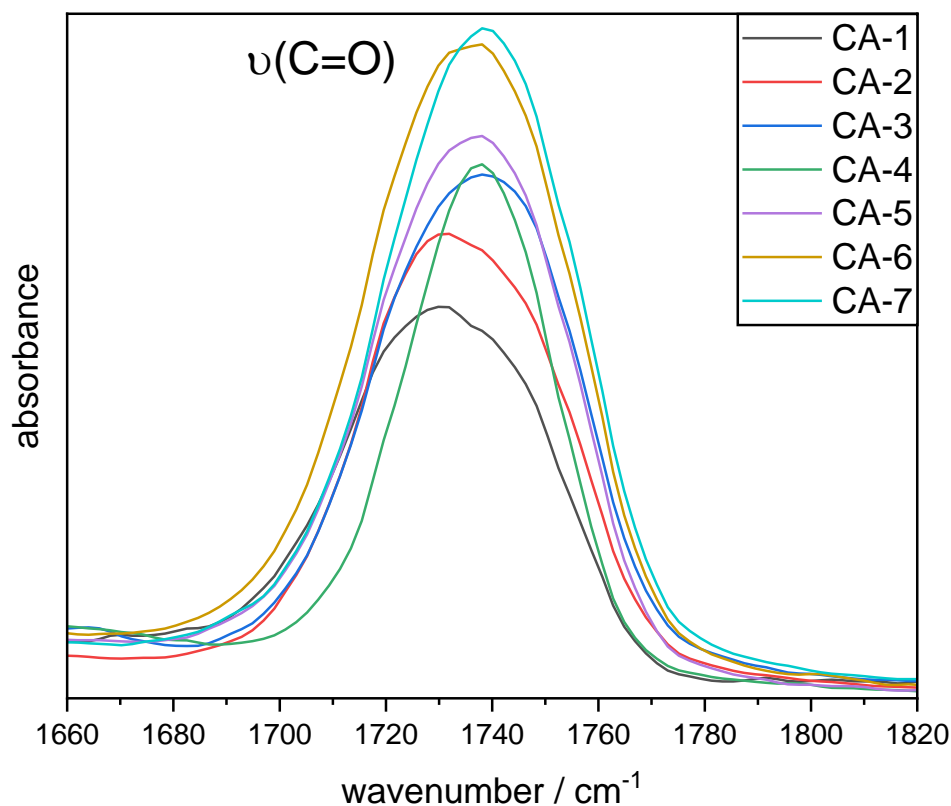
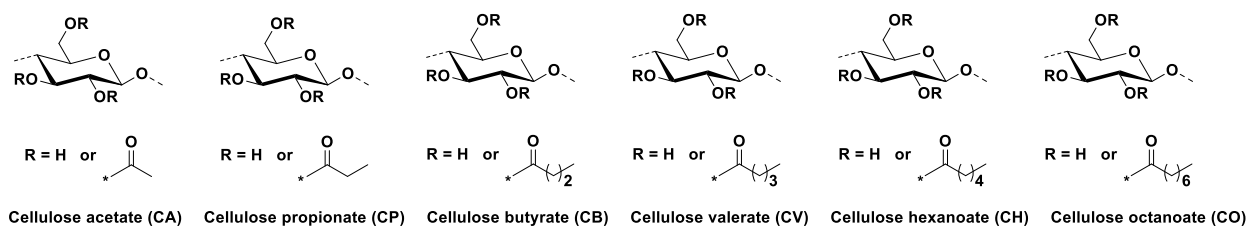


**Figure 1.** Expanded view of the C=O stretching vibration band for CA1 – 7 during the optimization process.

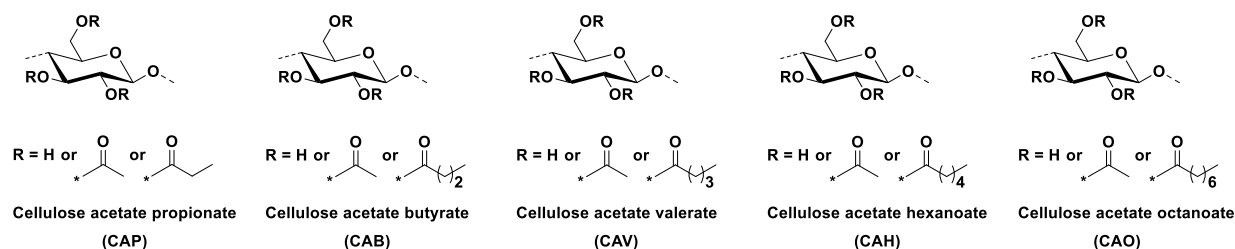
Just recently, Zhu *et. al.* published a rapid microwave assisted acylation approach for cellulose by using anhydrides in a CO<sub>2</sub> switchable solvent system.<sup>31</sup> Thus, as a second parameter, a different heating method, i.e. microwave heating, was applied. To our delight, CA-4 could be successfully synthesized within 10 minutes at 60 °C under microwave conditions, i.e. 300 W power input. Despite the short reaction time, CA-4 showed a more efficient modification (increased carbonyl vibration band at 1740 cm<sup>-1</sup> and DS<sub>1H</sub>, Figure 1 and Figure S5, respectively) compared to the former synthesized CAs, i.e. CA-1 to CA-3, under otherwise the same conditions. The latter phenomenon, i.e. higher DS at shorter reaction time, results from the improved heat transfer efficiency during

microwave irradiation.<sup>31</sup> Subsequently, the effect of different reaction temperatures (60 °C, 100 °C and 140 °C) was examined. As shown in Figure 1, a higher reaction temperature led to a significant increase of the carbonyl vibration band at around 1740 cm<sup>-1</sup>. Hence, it was not surprising that CA-6 (140 °C) possessed the highest DS<sub>1H</sub> (2.06, Figure S6), compared to CA-4 (60 °C) and CA-5 (100°C). In order to finalize the optimization process, VA and TMG equivalents were further increased (to 12.0/12.0 equiv.), as the influence of this parameter was not yet investigated under microwave conditions. At this point, a further increase of functionalization (DS<sub>1H</sub> = 2.34) could be detected and confirmed by IR and NMR spectroscopy (Figure 1, and Figure S7). Since the latter optimization step resulted in a minor improvement of DS<sub>1H</sub> (from 2.06 to 2.34, Table S1) and considering sustainability aspects, the investigated reaction conditions (Scheme 1) were applied for the subsequent synthesis of polymer libraries (Scheme 2). In the current work, two different polymer libraries of short chain CEs were synthesized by applying the previously described optimized reaction conditions (Scheme 2). Particularly, on the one hand, short chain CEs containing side chains with an equal length (using one specific vinyl ester as esterification reagent, Scheme 2A) and on the other hand, short chain mixed CEs including side chains with two different lengths (using VA and a second vinyl ester component as esterification reagent simultaneously, Scheme 2B).

A) Cellulose Esters



B) Mixed Cellulose Esters



**Scheme 2.** Libraries of synthesized short chain (mixed) CEs in a DMSO/TMG/CO<sub>2</sub> switchable solvent system.

Initially, the structural characterization of all short chain (mixed) CEs shown in Scheme 2 was performed via IR and <sup>1</sup>H NMR spectroscopy (Figure 2 and Figure 3, respectively). For the synthesized short chain CEs, i.e. cellulose acetate (CA), cellulose propionate (CP), cellulose butyrate (CB), cellulose valerate (CV), cellulose hexanoate (CH) and cellulose octanoate (CO), characteristic stretching vibration bands appearing at ~1740 cm<sup>-1</sup> (C=O, Figure 2A) and 1160 - 1230 cm<sup>-1</sup> (C-O<sub>ester</sub>, Figure 2A) in the corresponding IR spectra confirmed the successful CE formation. Additionally, a stretching vibration band arising at 2800 – 3020 cm<sup>-1</sup>, which can be assigned to the CH<sub>3</sub> and CH<sub>2</sub> groups of the aliphatic side chains, underlines the success of the modification process. Furthermore, it was observed, that the intensity of the C-H stretching vibration bands (2800 – 3020 cm<sup>-1</sup>) increased with the increase of the aliphatic side chain length (Figure 2A).

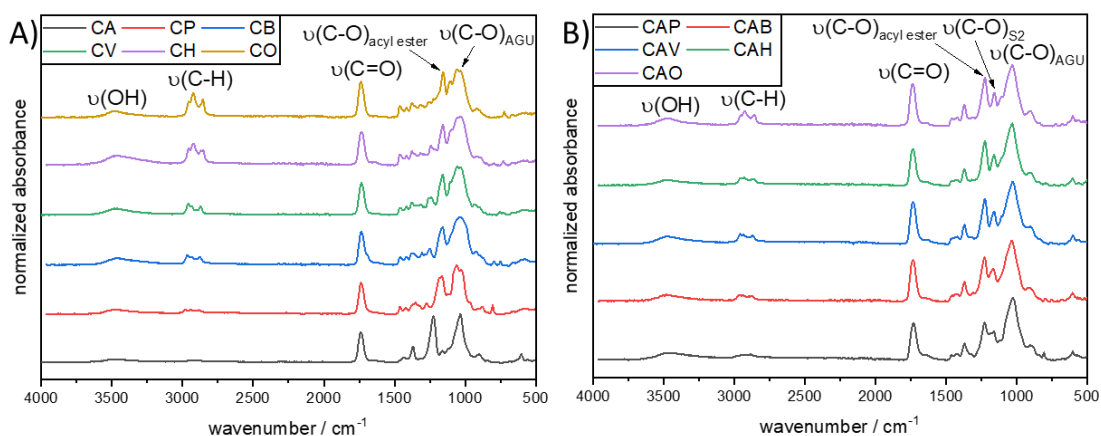


**Figure 2.** A) ATR-IR spectra of short chain CEs, i.e. CA (black line), CP (red line), CB (blue line), CV (green line), CH (violet line) and CO (yellow line). B) ATR-IR spectra of short chain mixed CEs, i.e. CAP (black line), CAB (red Line), CAV (blue line), CAH (green line) and CAO (violet line).

The aforementioned characterization procedure via IR spectroscopy including characteristic vibration bands at  $1740\text{ cm}^{-1}$  ( $\text{C}=\text{O}$ ),  $1160 - 1230\text{ cm}^{-1}$  ( $\text{C}-\text{O}_{\text{ester}}$ ) and  $2800 - 3020\text{ cm}^{-1}$  ( $\text{C}-\text{H}$ ) is also applicable for short chain mixed CEs (Figure 2B), i.e. cellulose acetate propionate (CAP), cellulose acetate butyrate (CAB), cellulose acetate valerate (CAV), cellulose acetate hexanoate (CAH) and cellulose acetate octanoate (CAO). However, as shown in Figure 2B, an additional vibration band arose at  $1155 - 1160\text{ cm}^{-1}$ , which can be associated to the C-O vibration of a supplemental structurally different ester moiety. Hence, the formation of short chain mixed cellulose esters containing ester side chains with two different chain lengths is confirmed by IR spectroscopy. In a complementary way,  $^1\text{H}$  NMR analysis was conducted for all synthesized short chain and mixed CEs. Figure 3 shows that all recorded NMR spectra display a similarity by revealing the unaffected anhydroglucose unit (AGU) protons from 2.91 to 5.20 ppm. Additional magnetic resonances at 1.80 – 2.13 ppm for CA and 2.04 – 2.42 ppm for CP, CB, CV, CH and CO can be associated to the protons in  $\alpha$ -position next to the ester moiety and thus show further evidence of successful CE formation. In the NMR spectra of mixed CEs containing two structurally different side chains (acetyl and a longer one), magnetic resonances at 1.80-2.13 ppm ( $-\text{O}-\text{C}(\text{CO})-\text{CH}_3$ ) and 2.04 – 2.42 ppm ( $-\text{O}-\text{C}(\text{CO})-\text{CH}_2-$ ) could be observed simultaneously. Hence, the

formation of short chain mixed CEs including acetyl and longer side chains ( $3 \leq C \leq 8$ ) is evidenced as well. As shown in Figure 3A and B,  $^1\text{H}$  NMR spectra of CEs and mixed CEs reveal additional magnetic resonances in the high field region (0.62 – 1.65 ppm) depending on the chain length of the employed vinyl esters.

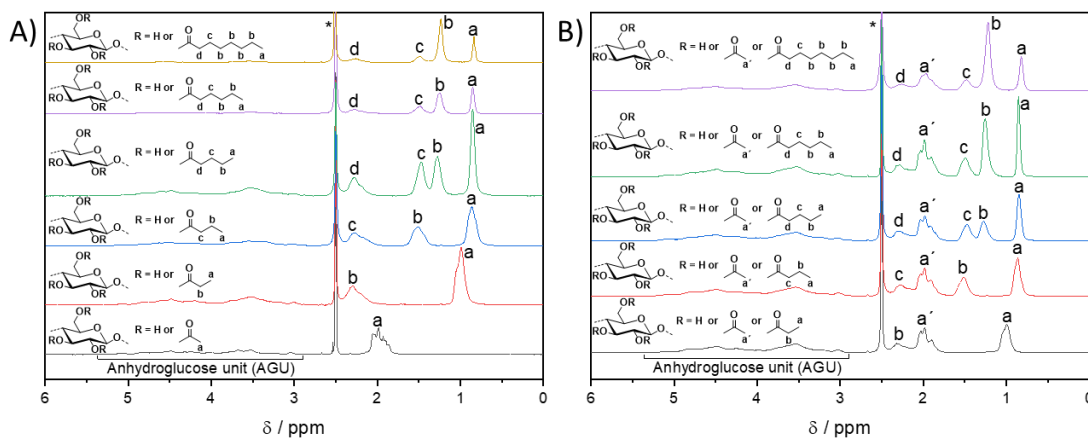


**Figure 3.** A)  $^1\text{H}$  NMR (400 MHz) of short chain CEs, i.e. CA (black line), CP (red line), CB (blue line), CV (green line), CH (violet line) and CO (yellow line), in  $\text{DMSO-}d_6$  (\*) at ambient temperature. B)  $^1\text{H}$  NMR (400 MHz) of short chain mixed CEs, i.e. CAP (black line), CAB (red line), CAV (blue line), CAH (green line) and CAO (violet line), in  $\text{DMSO-}d_6$  (\*) at ambient temperature.

In a complementary way,  $^{13}\text{C}$  NMR of CA and CAP were recorded as representative examples of all synthesized CEs and mixed CEs, respectively. In particular, characteristic magnetic resonances in the low-field region at 170, 169, and 168 ppm, which can be assigned to the quaternary carbon atom of the acyl groups at C6, C3 and C2 position, respectively, confirm the successful formation of CA (Figure S8). As shown in Figure S9, additional magnetic resonances at 173, 172 and 171 ppm attributable to the  $-\text{O-C(O)}-$  moiety of propyl ester side chains provide supplemental proof for the formation of mixed CEs, i.e. CAP. After this structural characterization, the DS of (mixed) CEs was determined according to literature known methodology via  $^1\text{H}$  NMR<sup>5</sup> in order to quantify the efficiency of the cellulose acylation approach in a  $\text{DMSO/TMG/CO}_2$  switchable solvent system. Although the current literature postulates that the maximal DS of cellulose derivatives decrease with increasing bulkiness of the attached side chains<sup>7</sup> this

phenomenon could not be observed in the existing system. Interestingly, CEs and mixed CEs were all obtained with DS in a similar range, i.e. from 2.05 to 2.16 and 1.99 to 2.16, respectively, as shown in Table 1, Figures S10 and Figure S11. It is also worth to mention that the incorporation ratio of VA and vinyl esters with increased chain length, i.e. vinyl propionate, vinyl butyrate, vinyl valerate, vinyl hexanoate and vinyl octanoate, in mixed CEs were determined via  $^1\text{H}$  NMR according to Eqn. 2 in the Supporting Information. Accordingly, it was observed that the incorporation of VA increased when an additional sterically hindered vinyl ester derivative was used. In other words, the relative content of VA in the corresponding mixed CEs increased from 53% for CAP to 61% for CAO (Figure S11). Compared to  $\text{CO}_2$ -based switchable solvent systems containing superbases like DBU and TBD, the DS of acylation seems to be limited when using TMG, likely a result of two main reasons. On the one hand, TMG can undergo an amidation reaction with vinyl esters, due to its increased nucleophilicity at the N atom of the imine functionality (confirmed by  $^1\text{H}$  NMR and GC-MS, Figure S12 and Figure S13, respectively).<sup>39</sup> On the other hand, the active H atom ( $-\text{C}=\text{NH}$ ) of TMG enables hydrogen bond formation among the TMG molecules, which lowers the deprotonation efficiency towards MCC drastically compared to DBU and TBD.<sup>39</sup> Nevertheless, comparable and high DS could efficiently be obtained, enabling the investigation of structure property relationships.

**Table 1.** Molecular and thermal characterization data of short chain (mixed) CEs.

Sample	DS <sub>1H</sub> <sup>a</sup>	Yield (%) <sup>b</sup>	$M_n$ (kDa) <sup>c</sup>	$\bar{D}^c$	$T_{d,5\%}$ (°C)
CA	2.34	73	59	2.3	264
CP	2.15	47	65	2.2	299
CB	2.17	58	116	2.2	292
CV	2.05	46	53	2.1	325
CH	2.17	46	102	2.2	333
CO	2.16	52	77	2.4	291
CAP	2.11	61	97	2.1	309
CAB	2.13	47	104	2.1	284
CAV	1.99	39	82	2.0	300
CAH	2.16	58	80	2.2	308
CAO	2.09	41	100	2.1	305

<sup>a</sup>Determined for CEs and mixed CEs via  $^1\text{H}$  NMR according to Eqn. (3) and (4) in SI, respectively; <sup>b</sup> determined gravimetrically; <sup>c</sup> obtained by HFIP SEC

Homogenous cellulose modification in CO<sub>2</sub>-based switchable solvent systems is known for the mild reaction conditions compared to the industrially employed heterogenous counterparts.<sup>7</sup> Hence, less of cellulose backbone degradation was indeed observed for homogenous modification approaches.<sup>5</sup> Size exclusion chromatography (SEC) confirmed high molecular weights for all synthesized CEs, i.e. 53 kDa <  $M_n$  < 102 kDa (Table 1 and Figure 4A), and mixed CEs, i.e., 82 kDa <  $M_n$  < 104 kDa (Table 1 and Figure 4B). For the mixed short chain CEs, multimodal SEC traces were observed, most likely due to inhomogeneous distribution of the two different acyl side chains. In addition to the so far presented structural characterization, materials properties play an important role in polymer materials in terms of potential industrial applicability. First, the decomposition temperatures, defined as the temperatures at which 5% weight loss occurs were determined by thermogravimetric analysis (TGA) measurements. All synthesized (mixed) CEs revealed a single major degradation step in the range of 200 to 400 °C, which can be assigned to the pyrolytic decomposition of the polymer chain skeleton. As shown in Figure S14, CA reveals a lower degradation temperature ( $T_{d,5\%} = 264$  °C) compared to native cellulose ( $T_{d,5\%} = 316$  °C), due to decreased intra- and intermolecular interactions. An increase of the side chain length from C=2 (CA) to C=6 (CH) resulted in a rise of  $T_{d,5\%}$  up to 333 °C (Figure S14). However, the aforementioned trend was not continued by CO, which showed a lower degradation temperature ( $T_{d,5\%} = 291$  °C). Mixed CEs showed degradation temperatures in a similar range from 300 °C (CAV) to 308 °C (CAP) except for CAB, which possesses a lower one ( $T_{d,5\%} = 284$  °C, Figure S15). Complementary to TGA, differential scanning calorimetry (DSC) measurements were conducted for all CEs and mixed CEs. An amorphous state for all synthesized CEs in a temperature range of -20 to 250 °C by only revealing glass transitions (Figure 4C and D) was observed. Thus, thermal characteristics are stated by the corresponding glass transition temperatures ( $T_g$ ). According to the internal plasticizer effect already known from literature,<sup>3</sup> it was found that  $T_g$  decreased with increasing side chain length from 203 °C (CA) to 172 °C (CB) for CEs and from 204 °C (CAP) to 177 °C (CAO) for mixed CEs. An increased molecular size of n-alkyl side groups increasingly limits the formation of inter- and intramolecular interactions (here hydrogen bonding of the cellulose backbone) and hence promotes backbone motion.<sup>31,40,41</sup> For CV, CH, and CO, no thermal transitions were observed, which can be attributed to the poor cellulose backbone



interactions. More precisely, due to the limited inter- and intramolecular interactions, i.e. hydrogen bonding, in CV, CH, and CO, a  $T_g$  was not detectable for these polymers.

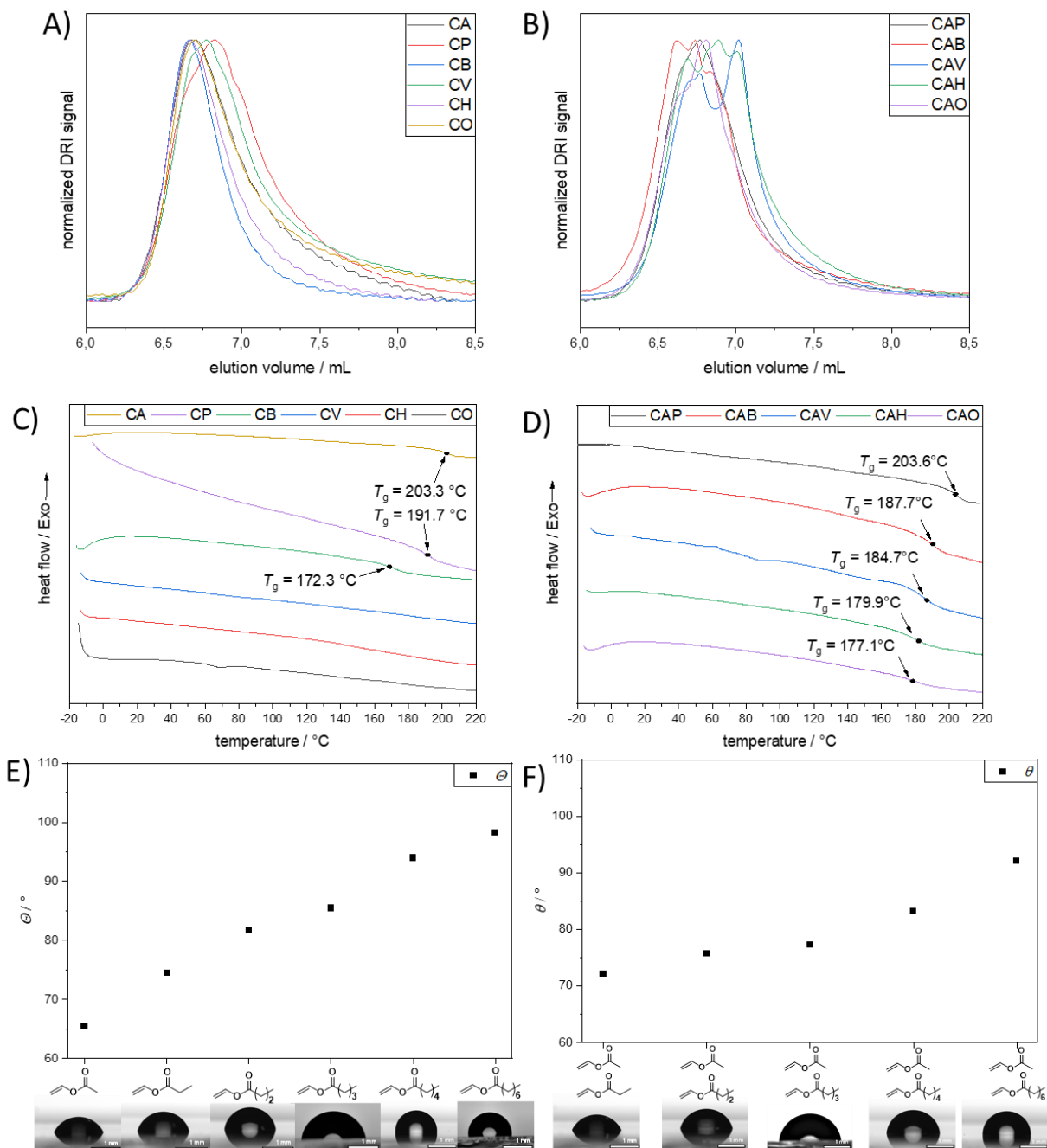


**Figure 4.** A) SEC traces of short chain CEs, i.e., CA (black line), CP (red line), CB (blue line), CV (green line), CH (violet line and CO (yellow line), in HFIP + 0.1% w/v KTFA. B) SEC traces of short chain mixed CEs, i.e., CAP (black line), CAB (red line), CAV (blue line), CAH (green line)

and CAO (violet line) in HFIP + 0.1% w/v KTFA. C) DSC studies (second heating run) of short chain CEs, i.e., CA (yellow line), CP (violet line), CB (green line), CV (blue line), CH (red line) and CO (black line) from  $-20^{\circ}\text{C}$  to  $220^{\circ}\text{C}$  with a heating rate of  $20^{\circ}\text{C min}^{-1}$  under a nitrogen flow. D) DSC studies (second heating run) of short chain mixed CEs, i.e., CAP (black line), CAB (red line), CAV (blue line), CAH (green line) and CAO (violet line) from  $-20^{\circ}\text{C}$  to  $220^{\circ}\text{C}$  with a heating rate of  $20^{\circ}\text{C min}^{-1}$  under a nitrogen flow. E) Static WCA measurements of short chain CEs at ambient conditions. F) Static WCA measurements of short chain mixed CEs at ambient conditions.

In addition to thermal characterization, the wettability properties of the synthesized materials were investigated by static water contact angle (WCA) measurements. Current literature postulates that particularly the introduction of long alkyl side chains, such as fatty acids, as well as the DS results in a significant influence regarding the hydrophobicity of CEs. Nevertheless, as to our knowledge, the dependence of WCA on the side chain length is only reported for long chain cellulose esters ( $C \geq 6$ ) containing low DS.<sup>42</sup> Therefore, the structure-property relationship of side chain length and hydrophobicity was studied separately for short chain CEs ( $2 \leq C \leq 8$ ) and short chain mixed CEs ( $2 \leq C \leq 8$ ). The incorporation of longer alkyl side chains resulted in a linear increase of WCA, i.e. in hydrophobicity, for short chain CEs and short chain mixed CEs (Figure 4E and F, respectively). More specifically, the WCA of short chain CEs increased from  $65^{\circ}$  for CA to  $98^{\circ}$  for CO ( $\Delta\text{WCA} = 33^{\circ}$ , Figure 4E) and of short chain mixed CEs from  $72^{\circ}$  for CAP to  $92^{\circ}$  for CAO ( $\Delta\text{WCA} = 20^{\circ}$ , Figure 4F). Subsequently, tensile strength measurements of mixed short chain cellulose esters, i.e. CAP to CAO, have been performed (Figure 5). According to the previously described internal plasticizer effect, it was observed that the Young's moduli of the respective materials decreased with increasing length of the second incorporated ester side chain from 13.6 MPa for CAP to 7.51 MPa for CAO (Figure 5). On a molecular level, the incorporation of longer side chains decreases intra- and intermolecular interactions between the cellulose backbones, i.e. mainly hydrogen bonding, and thus leads to a loss in the Young's modulus.

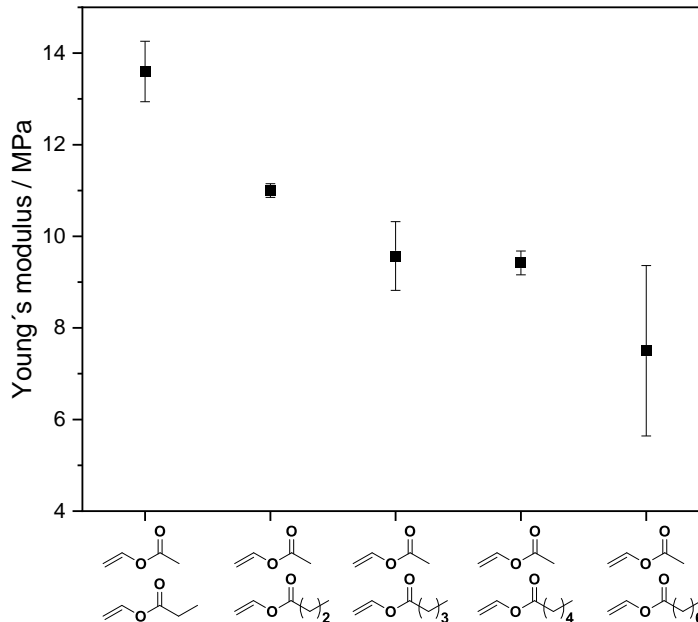


**Figure 5.** Young's moduli of mixed short chain cellulose esters at ambient conditions.

## CONCLUSION

In the present work, a rapid homogeneous microwave assisted synthesis of short-chain (mixed) CEs with high molecular weight ( $59 \text{ kDa} \leq M_n \leq 116 \text{ kDa}$ ) and variable acyl side chain length ( $2 \leq C \leq 8$ ) was developed in a DMSO/TMG/ $\text{CO}_2$  switchable solvent system. Thus, TMG was first implemented into the switchable solvent concept for cellulose esterification as a cheap and nontoxic alternative superbase. Upon the quantitative dissolution of cellulose and the optimization of the subsequent transesterification reaction with VA, two polymer libraries including short chain CEs and short chain mixed CEs were synthesized. In-depth structural characterization of (mixed) CEs via IR,  $^1\text{H}$  NMR,  $^{13}\text{C}$  NMR and SEC confirmed the successful formation within 10 minutes. The homogenous modification approach yielded (mixed) CEs with similar DS, i.e.,  $2.05 \leq \text{DS} \leq 2.34$  (CEs) and  $1.99 \leq \text{DS} \leq 2.16$  (mixed CEs), which affords a comparability of materials properties. Thus, in order to understand structure property relationships, all synthesized CEs were investigated regarding their thermal characteristics (via DSC and TGA) and wettability (via WCA). For mixed short chain cellulose esters, mechanical properties (tensile strength) decreased with increasing length of the side chain.

## ASSOCIATED CONTENT

The following files are available free of charge.

Additional DS and yield calculations, DS overviews, <sup>1</sup>H NMR, GC-MS and TGA analysis (PDF).

## AUTHOR INFORMATION

### Corresponding Author

**Michael A. R. Meier** – Institute of Biological and Chemical Systems – Functional Molecular Systems (IBCS-FMS), Karlsruhe Institute of Technology (KIT), 76131 Karlsruhe, Germany; Institute of Organic Chemistry (IOC), Materialwissenschaftliches Zentrum (MZE), Karlsruhe Institute of Technology (KIT), Straße am Forum 7, 76131 Karlsruhe, Germany

### Author

**Timo Sehn** - Institute of Biological and Chemical Systems – Functional Molecular Systems (IBCS-FMS), Karlsruhe Institute of Technology (KIT), 76131 Karlsruhe, Germany

### Funding Sources

n.a.

## Notes

The authors declare no conflict of interest.

## ACKNOWLEDGMENT

The authors acknowledge Prof. P. Levkin (WCA), Soft Matter Synthesis Laboratory (SML), i.e., Prof. P. Théato, Prof. J. Lahann and Prof. S. Bräse (DSC and TGA), and Prof. A. Colsmann (spin coating) for the access of diverse analytical characterization facilities.

## ABBREVIATIONS

CEs, cellulose esters, DMSO, dimethyl sulfoxide, TMG, tetramethylguanidine, CO<sub>2</sub>, carbon dioxide, ATR, attenuated total reflection, IR, infrared, NMR, nuclear magnetic resonance, *T<sub>g</sub>*, glass transition temperature, WCA, water contact angle, DS, degree of substitution, DMSO-TBAF, dimethyl sulfoxide-tetrabutylammonium fluoride, DMAc-LiCl, *N,N*-dimethylacetamide-lithiumchloride, ILs, ionic liquids, BMIMCl, 1-butyl-3-methylimidazolium chloride, EmimOPy, 1-ethyl-3-methylimidazolium 2-pyridinolate, DBU, 1,8-diazabicyclo[5.4.0]undec-7-en, TBD,

1,5,7-triazabicyclo[4.4.0]dec-5-en, CC, cellulose carbonate, CEC, cyanoethyl cellulose, CTEs, cellulose triesters, MCC, microcrystalline cellulose, AGU, anhydroglucose unit, CA, cellulose acetate, CP, cellulose propionate, CB, cellulose butyrate, CV, cellulose valerate, CH, cellulose hexanoate, CO, cellulose octanoate, CAP, cellulose acetate propionate, CAB, cellulose acetate butyrate, CAV, cellulose acetate valerate, CAH, cellulose acetate hexanoate, CAO, cellulose acetate octanoate, SEC, size exclusion chromatography, HFIP, hexafluoroisopropanol, KTFA, potassium trifluoroacetate, DSC, differential scanning calorimetry, GC-MS, gas chromatography – mass spectroscopy, TGA, thermogravimetric analysis,  $M_n$ , number average of molar mass, kDa, kilodalton,  $T_d$ , degradation temperature.

## REFERENCES

---

- 1 Stevens, C.; Verhe, R. *Renewable Bioresources: Scope and Modification for Non-Food Applications*, John Wiley & Sons, 2004, ISBN: 978-0-470-85446-4.
- 2 Fuyuno, I. Plastic promises. *Nature* **2007**, *446* (7137), 715-715.
- 3 Shukichi, T.; Tadahisa I.; Masatoshi, I. Long/Short Chain Mixed Cellulose Esters: Effects of Long Acyl Chain Structures on Mechanical and Thermal Properties. *ACS Sustainable Chem. Eng.*, **2017**, *5*, 1485-1493.
- 4 Klemm, D.; Heublein, B.; Fink, H. P.; Bohn, A. *Angew. Chem., Int. Ed.*, **2005**, *44*, 3358-3393.
- 5 Wolfs, J.; Meier, M. A. R. A more sustainable synthesis approach for cellulose acetate using the DBU/CO<sub>2</sub> switchable solvent system. *Green Chem.*, **2021**, *23*, 4410-4420.
- 6 Zhao, X.; Anwar, I.; Zhang, X.; Pellicciotti, A.; Storts, S.; Nagib, D. A.; Vodovotz, Y. Thermal and Barrier Characterizations of Cellulose Esters with Variable Side-Chain Lengths and Their Effect on PHBV and PLA Bioplastic Film Properties. *ACS Omega* **2021**, *6*, 24700-24708.

---

7 Esen, E.; Hadinger, P.; Meier, M. A. R. Sustainable Fatty Acid Modification of Cellulose in a CO<sub>2</sub>-Based Switchable Solvent and Subsequent Thiol-Ene Modification. *Biomacromolecules* **2021**, *22*, 586-593.

8 Heinze, T.; Liebert, T. Unconventional methods in cellulose functionalization. *Prog. Polym. Sci.*, **2001**, *26*, 1689-1762.

9 Mi, S.; Yao, Z.; Liu, F.; Li, Y.; Wang, J.; Na, H.; Zhub, J. Homogeneous cyanoethylation of cellulose with acrylonitrile in a CO<sub>2</sub> switchable solvent. *Green Chem.*, **2022**, *24*, 8677-8684.

10 Chen, Z.; Zhang, J.; Xiao, P.; Tian, W.; Zhang, J. Novel Thermoplastic Cellulose Esters Containing Bulky Moieties and Soft Segments. *ACS Sustainable Chem. Eng.* **2018**, *6*, 4931-4939.

11 Kusuma, S. B. W.; Hirose, D.; Yoshizawa, A.; Szabó, L.; Ina, D.; Wada, N.; Takahashi, K. Direct Synthesis of Full-Biobased Cellulose Esters from Essential Oil Component  $\alpha,\beta$ -Unsaturated Aldehydes. *ACS Sustainable Chem. Eng.* **2021**, *9*, 8450-8457.

12 Carrera, G. V. S. M.; Raymundo, A.; Fernandes, F. M.; Jordão, N.; Sousa, I.; Nunes da Ponte, M.; Branco, L. C. Tetramethylguanidine-based gels and colloids of cellulose. *Carbohydr. Polym.* **2017**, *169*, 58-64.

13 S. Fischer, S., Thümmeler, K., Volkert, B., Hettrich, K., Schmidt, I., Fischer, K., *Macromol. Symp.* **2008**, *262*, 89-96.

14 Steinmeier, H. Chemistry of cellulose acetylation. *Macromol. Symp.* **2004**, *208*, 49-60.

15 Malm, C. J., Tanghe, L. J., Laird, B. C., Preparation of Cellulose Acetate ACTION OF SULFURIC ACID, UTC, **1946**, *38*, 77-82.

---

16 Heinze, T., Liebert, T., Celluloses and Polyoses/ Hemicelluloses, Elsevier B.V., 2012, *10*, 83-152.

17 Onwukamike, K. N.; Grelier, S.; Grau, E.; Cramail, H.; Meier, M. A. R. Critical Review on Sustainable Homogeneous Cellulose Modification: Why Renewability Is Not Enough. *ACS Sustainable Chem. Eng.*, **2019**, *7*, 1826-1840.

18 Fink, H. P.; Weigel, P.; Purz, H. J.; Ganster, J. Structure formation of regenerated cellulose materials from NMMO-solutions. *Prog. Polym. Sci.* **2001**, *26*, 1473-1524.

19 Dogan, H.; Hilmioglu, N. D. Dissolution of cellulose with NMMO by microwave heating. *Carbohydr. Polym.* **2009**, *75*, 90-94.

20 Heinze, T.; Dicke, R.; Koschella, A.; Kull, A. H.; Klohr, E.-A.; Koch, W. Effective preparation of cellulose derivatives in a new simple cellulose solvent. *Macromol. Chem. Phys.* **2000**, *201*, 627-631.

21 Fischer, S.; Thümmeler, K.; Pfeiffer, K.; Liebert, T.; Heinze, T. Evaluation of molten inorganic salt hydrates as reaction medium for the derivatization of cellulose. *Cellulose* **2002**, *9*, 293-300.

22 El Seoud, O. A.; Marson, G. A.; Ciacco, G. T.; Frollini, E. An efficient, one-pot acylation of cellulose under homogeneous reaction conditions. *Macromol. Chem. Phys.* **2000**, *201*, 882-889.

23 McCormick, C. L.; Callais, P. A.; Hutchinson, B. H. Solution studies of cellulose in lithium chloride and *N,N*-dimethylacetamide. *Macromolecules* **1985**, *18*, 2394-2401.

24 Zhang, H.; Wu, J.; Zhang, J.; He, J. 1-Allyl-3-methylimidazolium Chloride Room Temperature Ionic Liquid: A New and Powerful Nonderivatizing Solvent for Cellulose. *Macromolecules* **2005**, *38*, 8272-8277.

---

25 Wu, J.; Zhang, J.; Zhang, H.; He, J.; Ren, Q.; Guo, M. Homogeneous Acetylation of Cellulose in a New Ionic Liquid. *Biomacromolecules* **2004**, *5*, 266-268.

26 Swatloski, R. P.; Spear, S. K.; Holbrey, J. D.; Rogers, R. D. Dissolution of Cellulose with Ionic Liquids. *J. Am. Chem. Soc.* **2002**, *124*, 4974-4975.

27 Xie, H.; Yu, X.; Yang, Y.; Zhao, Z. K. Capturing CO<sub>2</sub> for cellulose dissolution. *Green Chem.* **2014**, *16*, 2422-2427.

28 Zhang, Q.; Oztekin, N. S.; Barrault, J.; De Oliveira Vigier, K.; Jérôme, F. Activation of Microcrystalline Cellulose in a CO<sub>2</sub>-Based Switchable System. *ChemSusChem*. **2013**, *6*, 593-596.

29 Jessop, P. G.; Heldebrant, D. J.; Li, X.; Eckert, C. A.; Liotta, C. L. Reversible nonpolar-to-polar solvent. *Nature*, **2005**, *436*, 1102–1102.

30 Onwukamike, K. N.; Grelier, S.; Grau, E. Cramail, H.; Meier, M. A. R. Sustainable Transesterification of Cellulose with High Oleic Sunflower Oil in a DBU-CO<sub>2</sub> Switchable Solvent. *ACS Sustainable Chem. Eng.* **2018**, *6*, 8826-8835.

31 Yao, Z.; Mi, S.; Chen, B.; Liu, F.; Na, H.; Zhu, J. Rapid Homogeneous Acylation of Cellulose in a CO<sub>2</sub> Switchable Solvent by Microwave Heating. *ACS Sustainable Chem. Eng.* **2022**, *10*, 17327-17335.

32 Söyler, Z.; Onwukamike, K. N.; Grelier, S.; Grau, E.; Cramail, H.; Meier, M. A. R. Sustainable succinylation of cellulose in a CO<sub>2</sub>-based switchable solvent and subsequent Passerini 3-CR and Ugi 4-CR modification. *Green Chem.* **2018**, *20*, 214-224.



---

33 Onwukamike, K. N.; Tassaing, T.; Grelier, S.; Grau, E.; Cramail, H.; Meier, M. A. R. Detailed Understanding of the DBU/CO<sub>2</sub> Switchable Solvent System for Cellulose Solubilization and Derivatization. *ACS Sustainable Chem. Eng.* **2018**, *6*, 1496-1503.

34 Wolfs, J.; Nickisch, R.; Wanner, L.; Meier, M. A. R. Sustainable One-Pot Cellulose Dissolution and Derivatization via a Tandem Reaction in the DMSO/DBU/CO<sub>2</sub> Switchable Solvent System. *J. Am. Chem. Soc.* **2021**, *143*, 18693-18702.

35 Kulomaa, T.; Matikainen, J.; Karhunen, P.; Heikkilä, M.; Fiskaria, J.; Kilpeläinen, I. Cellulose fatty acid esters as sustainable film materials – effect of side chain structure on barrier and mechanical properties. *RSC Adv.* **2015**, *5*, 80702-80708.

36 Jebrane, M.; Terziev, N.; Heinmaa, I. Biobased and Sustainable Alternative Route to Long-Chain Cellulose Esters. *Biomacromolecules* **2017**, *18*, 498-504.

37 Joly, N.; Granet, R.; Branland, P.; Verneuil, B.; Krausz, P. New methods for acylation of pure and sawdust-extracted cellulose by fatty acid derivatives - Thermal and mechanical analyses of cellulose-based plastic films. *J. Appl. Polym. Sci.* **2005**, *97*, 1266-1278.

38 Crepy, L.; Chaveriat, L.; Banoub, J.; Martin, P.; Joly, N. Synthesis of Cellulose Fatty Esters as Plastics Influence of the Degree of Substitution and the Fatty Chain Length on Mechanical Properties. *ChemSusChem* **2009**, *2*, 165-170.

39 Wang, C.-G.; Li, N.; Wu, G.; Lin, T. T.; Lee, A. M. X.; Yang, S.-W.; Li, Z.; Luo, H.-K. Carbon Dioxide Mediated Cellulose Dissolution and Derivatization to Cellulose Carbonates in a Low-pressure System. *Carbohydr. Polym. Technol. Appl.* **2022**, *3*, 100186.

---

40 Morooka, T.; Norimoto, M.; Yamada, T. Dielectric Properties of Cellulose Acylates. *J. Appl. Polym. Sci.* **1984**, *29*, 3981-3990.

41 Danjo, T., Iwata, T. Syntheses of Cellulose branched ester derivatives and their properties and structure analyses. *Polymer*, **2018**, *137*, 358-363.

42 Willberg-Keyrilainen, P.; Vartiainen, J.; Harlin, A., Ropponen, J. The effect of side-chain length of cellulose fatty acid esters on their thermal, barrier and mechanical properties. *Cellulose* **2017**, *24*, 505-517.